

Temperature Dependent Valley Relaxation Dynamics in Single Layer WS₂ Measured Using Ultrafast Spectroscopy

Cong Mai,¹ Yuriy G. Semenov,² Andrew Barrette,¹ Yifei Yu,³ Zhenghe Jin,² Linyou Cao,^{3,*} Ki Wook Kim,^{2,†} and Kenan Gundogdu^{1,‡}

¹*Department of Physics, North Carolina State University, Raleigh, NC 27695, USA*

²*Department of Electrical and Computer Engineering,
North Carolina State University, Raleigh, NC 27695, USA*

³*Department of Material Science and Engineering,
North Carolina State University, Raleigh, NC 27695, USA*

Abstract

We measured the lifetime of optically created valley polarization in single layer WS₂ using transient absorption spectroscopy. The electron valley relaxation is very short (< 1 ps). However the hole valley lifetime is at least two orders of magnitude longer and exhibits a temperature dependence that cannot be explained by single carrier spin/valley relaxation mechanisms. Our theoretical analysis suggests that a collective contribution of two potential processes may explain the valley relaxation in single layer WS₂. One process involves direct scattering of excitons from K to K' valleys with a spin flip-flop interaction. The other mechanism involves scattering through spin degenerate Γ valley. This second process is thermally activated with an Arrhenius behavior due to the energy barrier between Γ and K valleys.

PACS numbers: 73.21.-b, 78.47.j-, 71.35.-y

INTRODUCTION

The discovery of graphene, a monolayer of carbon atoms, has inspired considerable interest in other 2D material systems in search of exotic electronic, optical and mechanical properties and novel practical applications[1–4]. In particular, two-dimensional transition metal dichalcogenides (TMDC) recently emerged as a promising material system with many potential electronic applications. With their tunable direct gap in visible range of the optical spectrum, absence of dangling bonds and high surface-to-volume ratio, these 2D semiconducting systems are ideal for field-effect transistors (FET), photovoltaics, light emitting diodes (LEDs), molecule sensing, and electrocatalytic water splitting applications[5–14]. Moreover, due to strong spin-orbit splitting they have been subject to specific spin and valley applications. The optical band gap in these structures are located at the K and $K' = -K$ points at the edge of the Brillouin zone. A strong spin-orbital coupling results in distinct states with different spin and valley indices so that K to K' elastic transition requires a spin flip for the electrons and holes. One immediate consequence of this property is the ability to control valley polarization, hence crystal quasi-momentum of electrons, by using circularly polarized light, which is impossible in conventional semiconductors due to negligible momentum of photons. This could open up opportunities for developing optoelectronic and valleytronic applications based on manipulation of spin and valley polarization of charge carriers[11–13, 15–17].

Detailed understanding of inter-valley relaxation dynamics is critical for the implementation of valleytronic applications. Very recently, numerous experimental and theoretical efforts have been devoted to characterization of electronic structure and optical properties of TMDCs[18–26]. However, there are only limited experimental studies that directly address the valley and spin relaxation process. Recently we measured valley lifetime in single layer MoS_2 to be 10 ps at 74K, using time-resolved absorption spectroscopy[27]. Surprisingly this relaxation time is very short, as large spin splitting in the valence band and spin valley coupling in K and K' valleys was expected to impede hole valley scattering[11–13, 15–17, 26, 27]. As of now an accurate picture of valley relaxation mechanisms in atomically thin TMDCs is missing. In the current work, we studied thermal dependence of valley relaxation of excitons in monolayer WS_2 using broadband transient absorption spectroscopy. In WS_2 the spin-orbit splitting is significantly larger compared to MoS_2 and other TMDCs

[13, 18–21]. Even so we observe that hole valley lifetime is more than an order of magnitude larger in WS₂ compared to MoS₂. Similar to MoS₂, electron valley relaxation is dominated by many body interactions and faster compared to hole valley relaxation. Based on temperature dependence of valley lifetimes, we propose a mechanism for an exciton-mediated valley relaxation process for holes in single layer WS₂.

In order to measure the valley relaxation time, we performed experiments on single layer WS₂ samples grown on quartz substrates using a chemical vapor deposition technique (Sup. Inf.)[29–32]. In time resolved experiments, circularly polarized 60 fs pump pulses, tuned to lower energy tail of A excitonic transition (1.977 eV) to create electron-hole pairs in the K valley. The differential transmission of a same circularly polarized (SCP) broad band white-light continuum probe pulse measures the relaxation within the same valley and opposite circularly polarized probe pulse (OCP) measures the population in the other valley. The decay of the polarization anisotropy between the SCP and the OCP spectra reveals the intervalley relaxation dynamics.

Figure 1 (a) schematically displays the electronic band structure for WS₂ at the K and K' points, adapted from Ref. [33]. The conduction band is composed by $d[1 - 3z^2]$ orbitals $|L, m\rangle$ of W with zero magnetic quantum number $m = 0$ under orbital moment $L = 2$ and relatively small admixture of $p[x - i\mathbf{y}]$ orbitals of S [17] with $m = -\nu$, which constitutes relatively small, 27 meV, spin splitting ($\nu = \pm 1$ corresponds to K and K' valleys). The valence band is formed by $d[(x + i\mathbf{y})^2]$ orbitals of W with $m = 2\nu$ and some admixture of p -orbitals of S that conditions much larger, 435 meV, valence band spin splitting [17, 18]. This spin splitting leads to energetically well separated A and B excitonic transitions shown by red and blue arrows in Fig. 1a. Their electro-dipole interband optical transitions are coupled with circularly polarized light.

Figure 1(b) shows transient SCP and OCP spectra for A exciton at 110 K. Initially the SCP spectrum shows a dispersive line shape in which the lower energy tail of the spectrum exhibits ground state bleaching (GSB) and stimulated emission (SE) and the higher energy tail exhibits photoinduced absorption (PIA). This dispersive feature evolves into purely absorptive line shape in about 7.6 ps. The OCP spectrum also exhibits a dispersive line shape, though less prominent than that of SCP. In the later time delays the anisotropy between the SCP and OCP spectra vanishes and a sharp dip shows up at 2.04 eV.

We attribute this dispersive distortion to phase-space filling effects similar to those ob-

served in conventional semiconductors[34, 35]. Briefly the photoexcited population blue-shifts the A exciton absorption, resulting in a differential line-shape in the transient spectrum. Monolayer materials exhibit ultra-tight quantum confinement[20, 21, 35]. Thus phase-space filling of carriers, which is related to Pauli-blocking, is very significant[26, 34, 35]. A similar blue shift has been observed in MoS_2 transient absorption studies as well[26]. The exact source of the spectral dip at 2.04 eV is unclear. It could be due to an overlapping absorptive transition from the excited state. A better understanding of the band structure and the excited states of the WS_2 is needed for analyzing this feature.

The evolution of the polarization anisotropy, measured by the difference between the SCP and OCP spectra in Figure 1, reveals the valley relaxation time of electrons and holes. The immediate presence of A exciton feature in the OCP spectra clearly suggests that a significant fraction of electron population, initially photo-excited in the K valley, quickly delocalize between K and K' valleys within 200 fs, which is within the time resolution of the experiment. This is because without any valley relaxation OCP should not exhibit any A exciton feature. The electron relaxation into the K' valley (i.e. transition of the direct exciton $[eK, hK]$, with both carriers in K -valley, to indirect one (dark exciton) $[eK', hK]$) leads to bleaching of the A exciton absorption in the OCP spectra. This immediate electron valley delocalization has been observed in single layer MoS_2 and attributed to coherent coupling of excitonic states[26]. While the circularly polarized optical transitions are valley specific, the resulting optically created exciton associated with a specific valley, K or K' , is not an eigenstate of the full exciton problem. Strong electron-hole confinement in exciton with energy 710 meV [37] and radius around 1 - 2 nm couples the K and K' valleys. As a result the electron in K valley quickly delocalizes over both valleys. This is further confirmed with the analysis of the evolution of the B exciton transition. As observed in Figure 2 (a, b), the B transition bleached immediately after the pump pulse in both SCP and OCP spectra with equal intensity. Because the B valence levels are very high in energy and are not populated with the pump pulse, it is only sensitive to electron dynamics. Hence electrons occupy B -levels in both valleys immediately upon photoexcitation. Because B -levels have opposite spin orientation; these spectra suggest not only that valley relaxation of the electrons is very quick but also that electron spin relaxation within the same valley is very fast (Fig. 2 c, d).

In contrast to fast conduction band spin and valley relaxation, hole delocalization is

not favorable energetically due to the large, $\Delta_{SO} \simeq 450$ meV, spin orbital splitting, which imposes the energy gap between the parallel spin states in the two valleys (Fig. 1a). Hence hole valley relaxation takes a much longer time. The total loss of the polarization anisotropy in the SCP and OCP spectra show that it is around 100 ps. We note that this is much longer compared to MoS₂ where the valley relaxation takes place in about 10 ps.

In order to resolve hole valley relaxation mechanism we performed transient absorption experiments in a range of temperatures from 74 K to 298 K. For each temperature, the pump pulses were tuned to the lower energy side of the *A* excitonic transition and resulting dynamics were probed with a broadband white light continuum pulse. At each temperature the early spectra show similar dynamics to 110 K data suggesting fast spin and valley relaxation dynamics for the electrons. However relaxation of the circularly polarized anisotropy clearly evolves at a different rate, revealing the thermal dependence of the hole valley relaxation dynamics.

In order to quantitatively extract the hole valley relaxation time, we analyzed the decay of polarization anisotropy at the *A* exciton transition by taking the difference of SCP and OCP spectra[38]. Neither single nor double exponential decay functions fit the anisotropy decay. Therefore we used a triple exponential fit. For all temperatures the first time constant is in 100 fs range, within the resolution of the experiment. The second time constant is in 1.5-3 ps range (Sup. Inf.). The slow component is the only one that exhibits clear temperature dependence varying from 88 ps to 8 ps at 74 K and 298 K respectively (Fig. 3). In the following this slow component is used for theoretical analysis of the valley relaxation process.

We considered several previously proposed inter-valley relaxation mechanisms to explain the experimental results. Our initial analysis suggests single carrier relaxation mechanisms cannot be responsible for the temperature dependence that we observe. For instance scattering with nonmagnetic impurities has been suggested as a potential valley relaxation process. Reference [39] shows that this mechanism requires a $\sim k^4$ dependence on hole momentum, which leads to a stronger temperature dependence (T^2) than our observation. Relaxation through flexural phonon modes was also considered as a potential mechanism[44]. It predicts an inverse relation between mobility and relaxation rate, and order of magnitude longer valley lifetimes compared to our results, hence it is unlikely to be responsible for the valley relaxation in WS₂.

We considered spin relaxation mechanisms such as Elliot-Yafet (EY) and Dyakonov-Perel

(DP) processes as well. These processes require scattering of carriers under inhomogeneous magnetic field. For instance in conventional semiconductors, Dresselhaus effect leads to such an effective field. Unlike many conventional semiconducting materials in TDMCs the spin quantization axis retains normal direction over all of Brillouin zone except the specific points where spin splitting reduces to zero. Such a property is clearly demonstrated in Ref. [17] based on calculations involving 80 energy bands of MoS₂. Our first principle calculations for WS₂ also reproduce the absence of transversal spin components over all of Brillouin zone. Thus the hole/electron diffusive motion cannot mix the states with opposite spin directions along the normal to layer plane (i.e. z axis). Therefore Elliot-Yafet and Dyakonov-Perel mechanisms are irrelevant.

Note however that in a realistic structure the spin quantization axis deviates from the normal direction due to inversion asymmetry induced by the substrate. Indeed, modeling the substrate induced asymmetry by an effective external electric field, we found the spin quantization axis deviates from z -direction. Proportionality of this deviation to quasi-momentum shift from extremum points represents the Rashba effect with Hamiltonian $H_R = \alpha_\varphi |\Delta \mathbf{k}|$, ($\Delta \mathbf{k} = \pm \mathbf{K} - \mathbf{k}$, φ is an angle between $\Delta \mathbf{k}$ and in-plane axis x), which in addition reveals trigonal anisotropy of α_φ in the vicinities of each \mathbf{K} and $\mathbf{K}' = -\mathbf{K}$ points. The correspondent spin-relaxation rate is,

$$\tau_s^{-1} = \frac{2}{\hbar^2} \left\langle \frac{\alpha_\varphi^2 \Delta \mathbf{k}^2 \tau_k}{\tau_k^2 \omega_{SO}^2 + 1} \right\rangle \quad (1)$$

where brackets mean thermal averaging, $\omega_{SO} = \Delta_{SO}/\hbar$, and τ_k is momentum relaxation time. Our first principle calculations estimate the Rashba constant mediated by potential drop ΔU between two sides of a layer. Averaging over angle φ , we find $\alpha = \beta \Delta U$, where $\beta \simeq 1.1 \cdot 10^{-10}$ cm, which results in an insignificant contribution ($\tau_s^{-1} \sim 10^{-16} \langle \tau_k^{-1} \rangle$) of this mechanism to intervalley spin relaxation even at $\Delta U = 100$ meV.

We conclude that the previously discussed single particle relaxation mechanisms are not sufficient to explain exciton intervalley relaxation. On the other hand, the excitonic electron-hole exchange interaction lifts orthogonality of spin states attributed to different valleys. This effect describes a minimal exciton spin Hamiltonian

$$H_0 = \frac{\tau}{2} \Delta_{SO} \sigma_z + \frac{\tau}{2} \delta_{SO} s_z + \Delta_{eh} \sigma \mathbf{s}, \quad (2)$$

where σ and \mathbf{s} are the Pauli matrixes for electron and hole spins, $\tau = \pm 1$ the valley index,

Δ_{SO} and δ_{SO} are the hole and electron spin splitting induced by spin-orbital interaction and Δ_{eh} is the strength of electron-hole exchange interaction. It is important to note that this interaction mixes the exciton spin states located in different valleys. This is because electro-dipole interband transitions occur between electronic states with same spin that generates electron-hole pair with opposite spin directions, i.e. with zero projections $s_z + \sigma_z = 0$. Thus the transitions between K and $-K$ excitons would be proportional to the spin flip-flop factor $T = |\langle \uparrow, \downarrow | \downarrow, \uparrow \rangle|^2$, where $|\downarrow, \uparrow\rangle$ corresponds to $s_z = -1/2$. If the spin-independent intervalley relaxation rate is $\tau_{KK'}^{-1}$, the net exciton relaxation rate will be

$$\tau_{ex}^{-1} = \tau_{KK'}^{-1} \frac{4\Delta_{eh}^2}{(\Delta_{SO} - \delta_{SO})^2 + 4\Delta_{eh}^2}. \quad (3)$$

Exciton scattering on any (not only spin-associated) local defects or phonons actualize such transitions. In contrast to free carriers, excitons are composed of band states involving those far away from the extremums K or K' , due to their short radius. These states admix the conduction band state $|2, 0\rangle$ to valence bands of both valley states which lifts their orthogonality. For instance, small deviation $\sim 0.1|K - K'|$ from extremum leads to non-negligible admixture of conduction band by a factor of about $\xi \sim 0.01$.

In addition to the excitonic flip-flop mechanism, carrier scattering through Γ -point could also contribute to the valley relaxation. Here the optically excited K -exciton scatters to an indirect one $[K_e(K'_e)\Gamma_h]$ and then to direct K' -exciton. This mechanism is not subjected to spin restrictions with factor in Eq. (3) due to zero spin-orbital splitting ($\Delta_{SO} = \delta_{SO} = 0$) at the Γ point. Moreover, since Γ state is composed from $|2, 0\rangle$ and $|1, 0\rangle$ orbitals, the $K - \Gamma$ overlap is substantially stronger than direct inter-valley overlap. On the other hand the difference $\Delta_{K\Gamma}^{ex}$ in direct exciton energy $E_{ex}[K_e K_h] = E_e(K) - E_v(K) - E_X(K)$ and indirect one $E_{ex}[K_e \Gamma_h] = E_e(K) - E_v(\Gamma) - E_X(K_e \Gamma_h)$ imposes a thermal activation process with Arrhenius-like temperature dependence

$$\tau_{K\Gamma}^{-1} = r_{K\Gamma} \exp(-\Delta_{K\Gamma}^{ex}/kT), \quad (4)$$

where $\Delta_{K\Gamma}^{ex} = E_v(K) - E_v(\Gamma) + E_X(K) - E_X(K_e \Gamma_h)$, the $E_{e(v)}(B)$ is the energy at the conduction (valence) B -band edge [$B = K, \Gamma$] and $E_X(K)$ and $E_X(K_e \Gamma_h)$ are the binding energies for direct and indirect excitons. Our first principal calculations (Sup. Inf.) give $E_v(K) - E_v(\Gamma) = 310\text{meV}$, which is slightly different from previous calculations[21]. In

the 2D Wannier-Mott exciton model the difference $E_X(K) - E_X(K_e\Gamma_h) = \Delta E_X$ basically stems from different reduced effective masses $\mu(K)$ and $\mu(\Gamma)$ so that $\Delta E_X = E_X(K)[1 - \mu(\Gamma)/\mu(K)]$ [38].

We estimated the reduced effective masses $\mu(K)$ and $\mu(\Gamma)$ based on our first principle energy band structure calculations (Sup. Inf.)[40–42]. The resulting binding energy difference between the direct K -exciton and indirect $[K_e(K'_e)\Gamma_h]$ exciton, $\Delta E_X \simeq -170$ meV, gives an energy barrier of $\Delta_{K\Gamma}^{ex} \simeq 140$ meV.

Quantitative estimation of $r_{K\Gamma}$, Δ_{eh} and $\tau_{KK'}^{-1}$ would be grounded on theory of exciton formation in TMDCs, which is not completed yet. Therefore we will treat these parameters as phenomenological ones. We observe that low-temperature thermal dependence of $\tau_{KK'}^{-1}$ (Fig. 3b) is similar to that of phonon-assistant momentum relaxation rate $\tau_p^{-1} = \tau_p^{-1}(T)$ calculated from first principles (Sup. Inf.)[43]. For free holes τ_h^{-1} can be approximated with $\tau_h^{-1}(T) = r_h[1 + (T/T_0)]$ at $r_h = 7.5 \cdot \text{ps}^{-1}$ and $T_0 \simeq 200$ K in wide range (70 K to 200 K) of temperatures. Adapting similar dependence for exciton momentum relaxation and combining $\tau_{e,h}^{-1}(T)$ with Eq. (4) the net result of both mechanisms describes the temperature dependence in the form

$$\tau_{ex}^{-1} = r_{KK'}(1 + T/T_0) + r_{K\Gamma} \exp(-\Delta_{K\Gamma}^{ex}/kT). \quad (5)$$

Fig. 3b shows that only two free parameters, $r_{KK'} = 0.01 \text{ ps}^{-1}$ and $r_{K\Gamma} = 24 \text{ ps}^{-1}$, describe all data with experimental accuracy.

To conclude, we present ultrafast valley relaxation dynamics measurements in monolayer WS_2 . The intervalley scattering lifetime in monolayer WS_2 is much longer than that of monolayer MoS_2 . The thermal dependence of the valley relaxation rate indicates that, due to strong exciton binding energy and exchange interaction, electron-hole spin flip-flop mechanism becomes an efficient spin relaxation channel. Because such excitonic relaxation mechanisms will not affect free carrier valley relaxation, we predict much longer valley lifetime for free carriers, which is important for future efforts in developing spintronic/valleytronic devices based on TMDCs.

KWK acknowledges the support from SRC/NRI SWAN.

* lcao2@ncsu.edu

† kwk@ncsu.edu

‡ kgundog@ncsu.edu

- [1] K. S. Novoselov, D. Jiang, F. Schedin, T. J. Booth, V. V. Khotkevich, S. V. Morozov, and A. K. Geim, Proc. Natl. Acad. Sci. U.S.A. **102**, 10451 (2005).
- [2] A. K. Geim, Science **324**, 1530 (2009).
- [3] S. Z. Butler, S. M. Hollen, L. Cao, Y. Cui, J. A. Gupta, H. R. Gutiérrez, T. F. Heinz, S. Hong, J. Huang, A. F. Ismach, E. Johnston-Halperin, M. Kuno, V. V. Plashnitsa, R. D. Robinson, R. S. Ruoff, S. Salahuddin, J. Shan, L. Shi, M. G. Spencer, M. Terrones, W. Windl, and J. E. Goldberger, ACS Nano **7**, 2898 (2013).
- [4] D. Jariwala, V. K. Sangwan, L. J. Lauhon, T. J. Marks, and M. C. Hersam, ACS Nano **8**, 1102 (2014).
- [5] Q. H. Wang, K. Kalantar-Zadeh, A. Kis, J. N. Coleman, and M. S. Strano, Nat. Nanotechnol. **7**, 699 (2012).
- [6] B. Radisavljevic, A. Radenovic, J. Brivio, J. V. Giacometti, and A. Kis, Nat. Nanotechnol. **6**, 147 (2011).
- [7] L. Britnell, R. M. Ribeiro, A. Eckmann, R. Jalil, B. D. Belle, A. Mishchenko, Y.-J. Kim, R. V. Gorbachev, T. Georgiou, S. V. Morozov, A. N. Grigorenko, A. K. Geim, C. Casiraghi, A. H. Castro Neto, and K. S. Novoselov, Science **340**, 1311 (2013).
- [8] R. S. Sundaram, M. Engel, A. Lombardo, R. Krupke, A. C. Ferrari, Ph. Avouris, and M. Steiner, Nano Lett. **13**, 1416 (2013).
- [9] F. K. Perkins, A. L. Friedman, E. Cobas, P. M. Campbell, G. G. Jernigan, and B. T. Jonker, Nano Lett. **13**, 668 (2013).
- [10] K. He, C. Poole, K. F. Mak, and J. Shan, Nano Lett. **13**, 2931 (2013).
- [11] A. Splendiani, L. Sun, Y. Zhang, T. Li, J. Kim, C.-Y. Chim, G. Galli, and F. Wang, Nano Lett. **10**, 1271 (2010).
- [12] K. F. Mak, C. Lee, J. Hone, J. Shan, and T. F. Heinz, Phys. Rev. Lett. **105**, 136805 (2010).
- [13] D. Xiao, G. B. Liu, W. Feng, X. Xu, and W. Yao, Phys. Rev. Lett. **108**, 196802 (2012).
- [14] Y. Yu, S. Huang, Y. Li, S. N. Steinmann, W. Yang, and L. Cao, Nano Lett., **14**, 553 (2014).

- [15] K. F. Mak, K. He, J. Shan, and T. F. Heinz, Nat. Nanotechnol. **7**, 494 (2012).
- [16] H. Zeng, J. Dai, W. Yao, D. Xiao, and X. Cui, Nat. Nanotechnol. **7**, 490 (2012).
- [17] T. Cao, G. Wang, W. Han, H. Ye, C. Zhu, J. Shi, Q. Niu, P. Tan, E. Wang, B. Liu and J. Feng, Nat. Commun. **3**, 887 (2012).
- [18] K. Kořmider and J. Fernandez-Rossier, Phys. Rev. B **87**, 075451 (2013).
- [19] H. R. Gutierrez, N. Perea-Lopez, A. L. Elas, A. Berkdemir, B. Wang, R. Lv, F. Lopez-Uras, V. H. Crespi, H. Terrones, and M. Terrones, Nano Lett. **13**, 3447 (2013).
- [20] H. Zeng, G.-B. Liu, J. Dai, Y. Yan, B. Zhu, R. He, L. Xie, S. Xu, X. Chen, W. Yao, and X. Cui, Sci. Rep. **3**, 1608 (2013).
- [21] Z. Y. Zhu, Y. C. Cheng and U. Schwingenschlogl, Phys. Rev. B **84**, 153402 (2011).
- [22] W. Zhao, Z. Ghorannevis, L. Chu, M. Toh, C. Kloc, P.-H. Tan, and G. Eda, ACS Nano **7**, 791 (2013).
- [23] A. M. Jones, H. Yu, N. J. Ghimire, S. Wu, G. Aivazian, J. S. Ross, B. Zhao, J. Yan, D. G. Mandrus, D. Xiao, W. Yao, and X. Xu, Nat. Nanotechnol. **8**, 634 (2013).
- [24] L. Sun, J. Yan, D. Zhan, L. Liu, H. Hu, H. Li, B. K. Tay, J.-L. Kuo, C.-C. Huang, D. W. Hewak, P. S. Lee, and Z. X. Shen, Phys. Rev. Lett. **111**, 126801 (2013).
- [25] H. Shi, R. Yan, S. Bertolazzi, G. Gao, A. Kis, D. Jena, H. Xing and L. Huang, ACS Nano **7**, 1072 (2013).
- [26] S. Sim, J. Park, J. Song, C. In, Y. Lee, H. Kim, and H. Choi, Phys. Rev. B **88**, 075434 (2013).
- [27] C. Mai, A. Barrette, Y. Yu, Y. G. Semenov, K. W. Kim, L. Cao, and K. Gundogdu. Nano Lett., **14**, 202 (2014).
- [28] Q. Wang, S. Ge, X. Li, J. Qiu, Y. Ji, J. Feng and D. Sun. ACS Nano **7**, 11087 (2013).
- [29] Y. Yu, S. Hu, L. Su, L. Huang, Y. Liu, Z. Jin, A. A. Purezky, D. B. Geohegan, K. W. Kim, Y. Zhang, L. Cao, arXiv:1403.6181 (2014)
- [30] Y. -H. Lee, L. L. Yu. H. Wang, W. J. Fang, X. Ling, Y. M. Shi, C. T. Lin, J. K. Huang, M. T. Chang, C. S. Chang, M. Dresselhaus, T. Palacios, L. J. Li, and J. Kong, Nano Lett. **13**, 1852 (2013).
- [31] S. Najmaei, Z. Liu, W. Zhou, X. Zou, G. Shi, S. Lei, B. I. Yakobson, J.-C. Idrobo, and P. M. Ajayan and J. Lou, Nat. Mater. **12**, 754 (2013).
- [32] A. M. van der Zande, P. Y. Huang, D. A. Chenet, T. C. Berkelbach, Y.M. You, G.-H. Lee, T. F. Heinz, D. R. Reichman, D. A. Muller and J. C. Hone, Nat. Mater. **12**, 554 (2013).

- [33] G. Sallen, L. Bouet, X. Marie, G. Wang, C. R. Zhu, W. P. Han, Y. Lu, H. Tan, T. Amand, B. L. Liu, and B. Urbaszek, Phys. Rev. B **86**, 081301, (2012).
- [34] Y. H. Lee, A. Chavez-Pirson, S. W. Koch, H. M. Gibbs, S. H. Park, J. Morhange, A. Jeffery, and N. Peyghambarian, Phys. Rev. Lett. **57**, 2446 (1986).
- [35] D. N. Christodoulides, I. C. Khoo, G. J. Salamo, G. I. Stegeman, and E. W. V. Stryland, Adv. Opt. Photonics **2**, 60 (2010).
- [36] A. Kuc, N. Zibouche, and T. Heine. Phys. Rev. B **83**, 245213 (2011).
- [37] N. Peyghambarian, H. M. Gibbs, J. L. Jewell, A. Antonetti, A. Migus, D. Hulin, and A. Mysyrowicz Phys. Rev. Lett. **53**, 2433 (1984).
- [38] B. Zhu, X. Chen, X. Cui, arXiv:1403.5108v1 (2014).
- [39] H. Lu, W. Yao, D. Xiao, S. Shen, Phys. Rev. Let. **110**, 016806, (2013).
- [40] P. Giannozzi et al., J. Phys.: Condens. Matter **21**, 395502 (2009).
- [41] A. Klein, S. Tiefenbacher, V. Eyert, C. Pettenkofer, and W. Jaegermann, Phys. Rev. B **64**, 205416 (2001).
- [42] H.-P. Komsa, and A.V. Krasheninnikov, Phys. Rev. B **88**, 085318 (2013).
- [43] X. Li, J., T. Mullen, Z. Jin, K.M. Borysenko, M. Buongiorno Nardelli, and K.W. Kim, Phys. Rev. B **87**, 115418 (2013)
- [44] Y. Song, and H. Dery. Phys. Rev. Let. **111**,026601, (2013).
- [45] K. C. Hall, K. Gündogdu, E. Altunkaya, W. H. Lau, M. E. Flatté, T. F. Boggess, J. J. Zinck, W. B. Barvosa-Carter, and S. L. Skeith, Phys. Rev. B **68**, 115311 (2003).
- [46] K. Zerrouati, F. Fabre, G. Bacquet, J. Bandet, J. Frandon, G. Lampel, and D. Paget, Phys. Rev. B **37**, 1334 (1988).
- [47] M. I. D'yakonov and V. I. Perel, Zh. Eksp. Teor. Fiz. 60, 1954 (1971) [Sov. Phys. JETP **38**, 1053].
- [48] Y. Yafet, Phys. Rev. **85**, 478 (1952).
- [49] R. J. Elliott, Phys. Rev. **96**, 266 (1954).

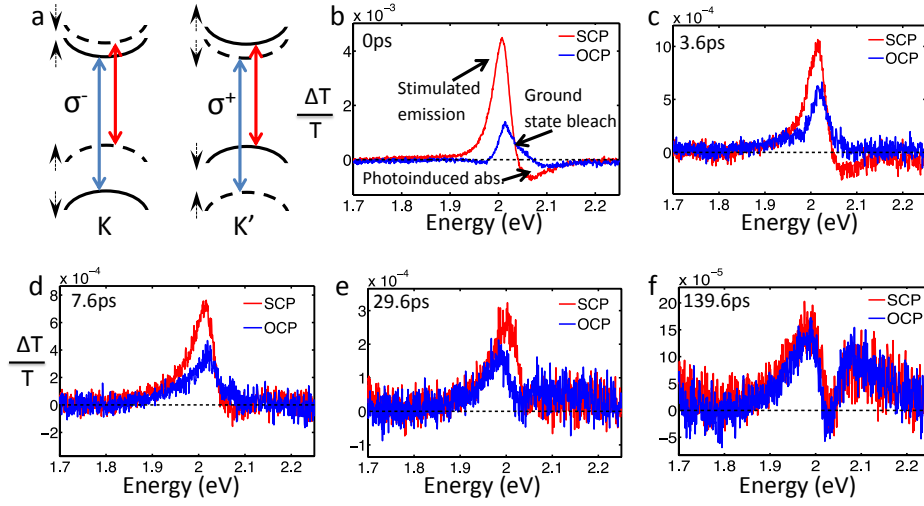


FIG. 1. (Color online) (a) Electronic structure and the optical transition at the K and K' points of monolayer WS₂. The dashed(solid) curves correspond to different spin states in A and B excitonic transitions. (b-f) Differential transmission at various delay at 110K for same (red) and opposite (blue) circularly polarized pump and probe pulses.

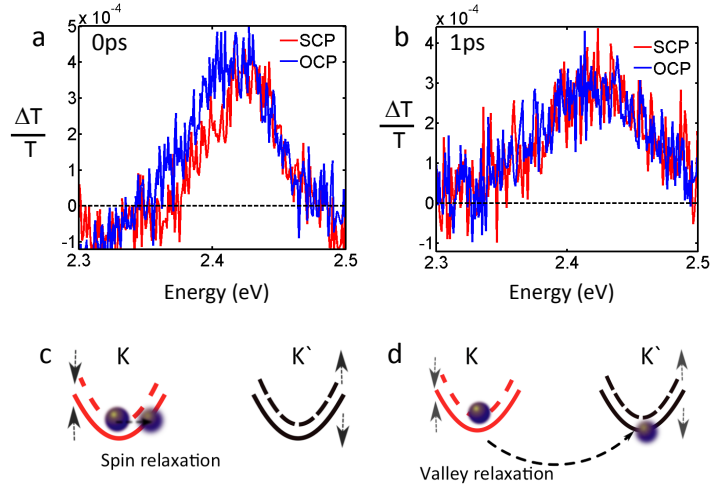


FIG. 2. (Color online) (a-b) Differential transmission of B exciton peak at various delay at 110K, 0fs (a) and 1ps (b) delays. Red is SCP and blue is OCP (c-d) Schematic illustration of spin and valley relaxation of electron.

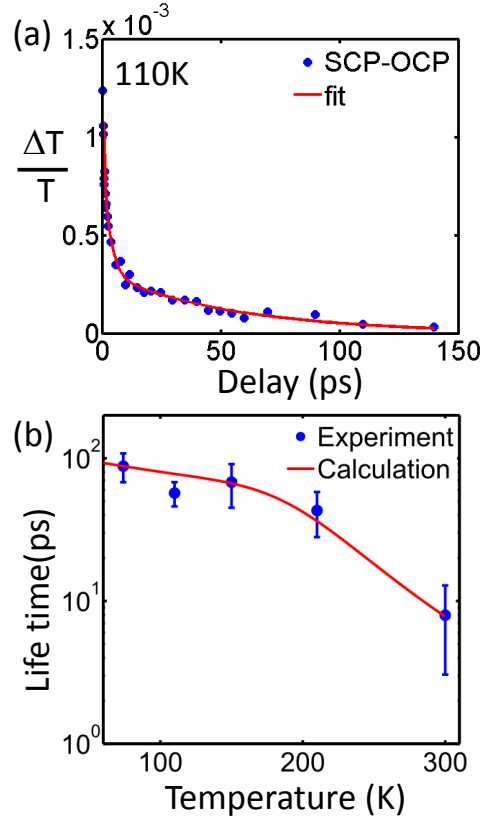


FIG. 3. (Color online) (a) time evolution of SCP-OCP peak intensity at 110 K and the fit to the three exponential decay function (solid line). (b) The temperature dependence of the slowest time constant.